

Distributed PMD Compensator in Lithium–Niobate–Tantalate: Performance Modeling Toward Highest Bit Rates

Suhas Bhandare, *Member, IEEE*, and Reinhold Noé, *Member, IEEE*

Abstract—Polarization mode dispersion (PMD) is caused by noncircular fiber cores and poses a serious threat for transmitting 10-Gb/s optical signals over older fibers and 40-Gb/s optical signals over any type of fiber. We study the architecture of a PMD compensator (PMDC) capable of 40-Gb/s operation in X -cut Y -propagation lithium niobate (LiNbO_3) based on cascaded integrated optical TE–TM mode converters with endlessly adjustable coupling phases and propose several improvements in its architecture to tailor its performance toward highest bit rates. The performance of such distributed PMDCs can be pushed toward highest bit rates of 160 and 640 Gb/s if they are implemented in mixed ferroelectric crystals such as lithium niobate tantalate ($\text{LiNb}_{1-y}\text{Ta}_y\text{O}_3$) or lithium tantalate (LiTaO_3) crystals, respectively. A tantalum (Ta) content y of up to 0.5 is good to realize a distributed PMDC for about 160-Gb/s operation. Two- and three-phase TE–TM mode converters for integrated optical PMD compensation are compared, and the latter are found to have slightly better electrooptic efficiency. For Z -cut lithium tantalate, four-phase electrodes which need only two independent operation voltages are found to be more attractive.

Index Terms—Guided wave optics, lithium niobate, lithium tantalate, polarization mode dispersion (PMD).

I. INTRODUCTION

POLARIZATION mode dispersion (PMD) is caused by noncircular fiber cores and limits capacity of optical trunk lines. It can be conveniently modeled as a concatenation of differential group delay (DGD) sections connected by variable polarization transformers. It can be compensated if appropriately oriented birefringence is added at the receiver side in reversed order. Therefore, a perfect PMD compensator (PMDC) shall consist of a large number of short DGD sections separated by variable polarization transformers. These polarization transformers would be adjusted so that the vectorial DGD profile of the PMDC should follow the DGD profile of the fiber transmission line in reverse order [1]. Implementation of such polarization transformers with endlessly adjustable coupling phases was proposed many years ago by Heismann and Ulrich [2]. A particularly suited material is X -cut Y -propagation lithium niobate (LiNbO_3) to implement such polarization transformers. Natural birefringence of this birefringent crystal cut (0.25 ps/mm) is oriented by electrooptical mode converters

and cancels the DGD [3]. This solution combines optimum performance and speed with a high degree of integration and, hence, low-cost potential. Since the function has already been demonstrated in [4], we now concentrate on design and performance optimization.

II. OPERATION PRINCIPLE

The operation principle is based on the spatially weighted coupling between two waves with slightly different propagation constants [2]. Two indicated waves might be propagating in two separate (noncoupled) waveguides, or they may represent two different modes (e.g., polarization modes) of a single mode optical waveguide. The phase difference between one mode and the coupled mode therefore depends on the position where coupling occurs and is periodic with the optical beat length $\Lambda = \lambda/\Delta n$. The TE–TM refractive index difference in a Ti-indiffused waveguide in X -cut Y -propagation lithium niobate is $\Delta n = 0.0679$ at a free space optical wavelength of $\lambda = 1550$ nm, thereby giving $\Lambda = 22$ μm . Interdigital electrodes are, therefore, needed for phase matching with a period equal to one optical beat length Λ . The widths and gaps of interdigital electrodes are set equal to one fourth of the optical beat length Λ , and subsequent electrode pairs are additionally spaced by three fourths of the optical beat length Λ , which allows mode coupling to be adjusted in both quadratures endlessly via the electrooptic coefficient r_{51} . The coupling coefficient κ is given by

$$\kappa \cong 2\hat{\Gamma}(\pi/2)n^3r_{51}(V/G)\lambda^{-1} \quad (1)$$

where $\hat{\Gamma}$ is a weighted field overlap integral factor, as defined later, and $n = 2.1785$ is the average refraction index of the waveguide. $r_{51} = 28$ pm/V is the relevant electrooptic coefficient, and V is the interelectrode voltage. The factor of two is introduced because of the push–pull effect of the interdigital electrodes.

Fig. 1 shows the schematic of such PMDC in the X -cut Y -propagation lithium niobate. Voltage $V_{1,i}$ acts on one set of comb electrodes and performs mode conversion in phase. Voltage $V_{2,i}$ acts on another set of comb electrodes, which are translated by three fourths of the optical beat length with respect to the first and performs mode conversion in quadrature. The resulting complex coupling coefficient κ is proportional to $V_{1,i} + jV_{2,i}$ for the i th in-phase and quadrature electrode pair.

Manuscript received December 6, 2006; revised March 22, 2007.

The authors are with the Optical Communication and High-Frequency Engineering Department, University of Paderborn, 33098 Paderborn, Germany (e-mail: suhas@ont.upb.de; noe@upb.de).

Digital Object Identifier 10.1109/JLT.2007.901515

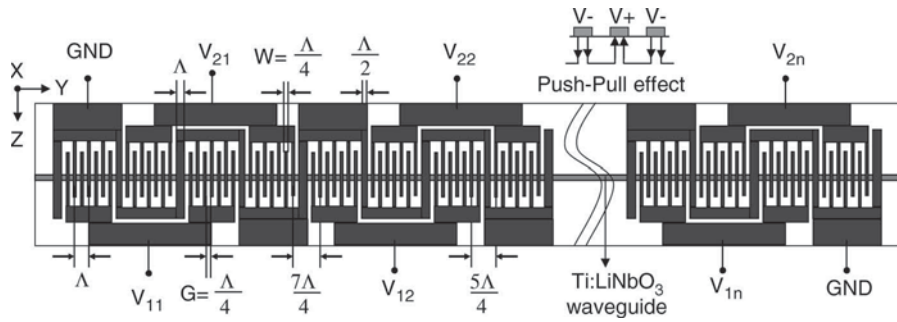


Fig. 1. Schematic of two-phase PMDC on X-cut Y-propagation lithium niobate.

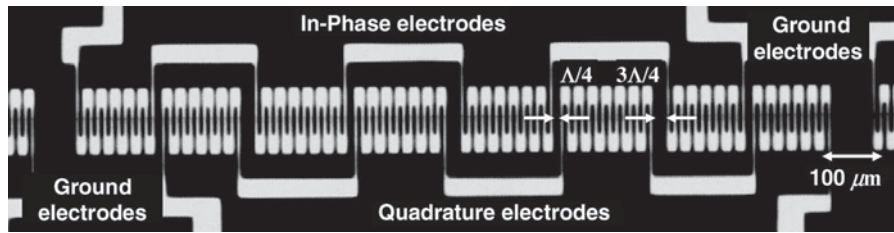


Fig. 2. Photograph of in-phase and quadrature TE-TM mode converter electrode pairs (in dark) on Ti:LiNbO₃ PMDC.

The need for two quadratures at least doubles the necessary chip length.

Fig. 2 shows a photograph of the portion of the chip used in [4]. The device was fiber pigtailed and packaged with slanted end faces to improve input/output optical return loss. Insertion loss was 4 dB, and polarization dependent loss (PDL) was 1.2 dB. Thermal tuning of the phase-matched wavelength was possible with 100 GHz/K coefficient.

To understand the device function, consider the *i*th electrode pair set with length $L_i = m\Lambda$, where *m* is an integer number of comb fingers in phase and quadrature electrodes, which together acts as an in-phase and quadrature mode converter. The overall Jones matrix of the waveguide section is the following:

$$\begin{bmatrix} \cos \varphi_i/2 & je^{-j\psi_i} \sin \varphi_i/2 \\ je^{j\psi_i} \sin \varphi_i/2 & \cos \varphi_i/2 \end{bmatrix} \quad (2)$$

with retardation $\varphi_i = 2L_i \sqrt{\kappa_{1,i}^2 + \kappa_{2,i}^2} : \sqrt{V_{1,i}^2 + V_{2,i}^2}$ and an orientation angle $\psi_i = \arg(\kappa_{1,i} + j\kappa_{2,i}) = \arg(V_{1,i} + jV_{2,i})$. The in-phase coupling coefficient κ_1 couples the linearly polarized eigenmodes with $\pm 45^\circ$, and the quadrature coupling coefficient κ_2 couples the right and left hand circularly polarized eigenmodes. Its eigenmodes lie on the S_2-S_3 great circle of the Poincaré sphere, with $S_2 + jS_3 = (V_{1,i} + jV_{2,i}) / \sqrt{V_{1,i}^2 + V_{2,i}^2}$. The Jones matrix of the DGD section is given by

$$\begin{bmatrix} e^{j\omega\tau_i/2} & 0 \\ 0 & e^{-j\omega\tau_i/2} \end{bmatrix} \quad (3)$$

where τ_i is the DGD of the *i*th section. In reality, the mode converter and DGD section cannot be separated; rather, they occur

jointly in the waveguide. Therefore, the whole device with *n* in-phase and quadrature electrode pairs acts like a cascade of alternating DGD sections and mode converters. In [1], it is shown that such a cascade

- 1) can produce DGDs from 0 to a maximum value given by the DGD in the absence of mode conversion;
- 2) can accommodate and endlessly track naturally occurring, typical PMD scenarios of transmission fiber better than other approaches with only few DGD sections or, worse, variable DGD sections.

Measured DGD profiles in [5], i.e., concatenations of local PMD vectors transformed into a common reference system, show the predicted completely versatile performance in practice as well. More theory about device function and DGD profiles is also given in [6].

The observed PDL is a bit higher than that of commercial LiNbO₃ devices such as modulators. It can be expected to come down in an industrial device fabrication. Since penalties for DGDs approaching one symbol duration are catastrophic, even the comparatively small PDL observed in the present device is tolerable, and successful operation has indeed been shown in [4].

III. TWO VERSUS THREE PHASES

As has been mentioned in [2], the two-phase implementation is not the only possible choice. If isolated electrode crossings are available, three-phase electrodes can be used with electrode widths and gaps equal to $\Lambda/6$. In phase and quadrature mode conversion can be produced by the linear combinations of the “sine” and “cosine” cases shown in Figs. 4 and 5. Even and odd voltage distributions are applied by choosing electrode voltages $V_0 f(\hat{y})$, where V_0 serves as a reference voltage, and \hat{y} is the longitudinal position of the middle of an

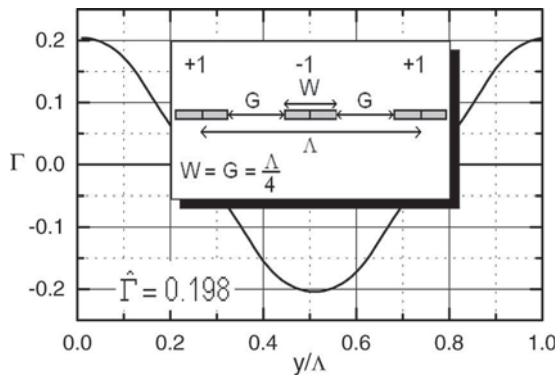


Fig. 3. Two-phase electrodes with corresponding driving voltages and local field overlap integral factors versus normalized local coordinate “ y .”

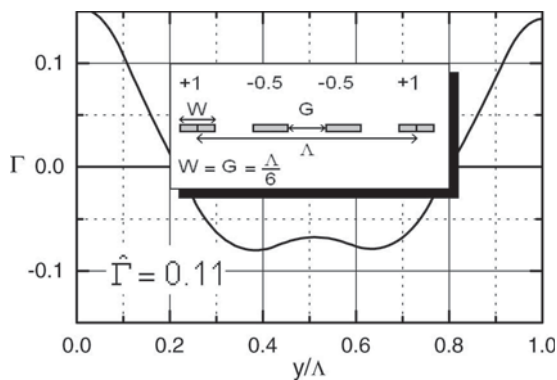


Fig. 4. Three-phase cosine electrodes with corresponding driving voltages and local field overlap integral factors versus normalized local coordinate “ y .”

electrode. Here, $f(y) = \cos(2\pi y/\Lambda)$ and $f(y) = \sin(2\pi y/\Lambda)$ are structure functions needed for cosine and sine cases, respectively.

The point matching method [7] has been chosen to calculate the electrostatic fields of these periodic electrode structures. The transversal optical field $\mathbf{E}_O(x, z)$ is assumed to be Gaussian and Hermite–Gaussian along width and depth of the single mode Ti-indiffused waveguide in LiNbO₃ with mode field diameters matched to our experimental values. The position-dependent overlap integral $\Gamma(y)$ [8] must be multiplied by $f(y)$, integrated over one beat length, and normalized to obtain the weighted overlap integral factor

$$\hat{\Gamma} = \frac{2}{\Lambda} \int_0^{\Lambda} \Gamma(y) f(y) dy$$

with

$$\Gamma(y) = \frac{G}{V} \cdot \frac{\iint |\mathbf{E}_O(x, z)|^2 \cdot E_x(x, y, z) \cdot dx dz}{\iint |\mathbf{E}_O(x, z)|^2 \cdot dx dz} \quad (4)$$

as defined in [9].

For cosine and sine cases, $\hat{\Gamma}$ is the real or imaginary part of the spatial Fourier coefficient of $\Gamma(y)$, respectively. $E_x(x, y, z)$ is the vertical component of the electrostatic field in the crystal. In $\Gamma(y)$, we have multiplied by the applicable gap G and divided by the maximum interelectrode voltage V , as defined above. Fig. 3 shows the local overlap integral factors $\Gamma(y)$

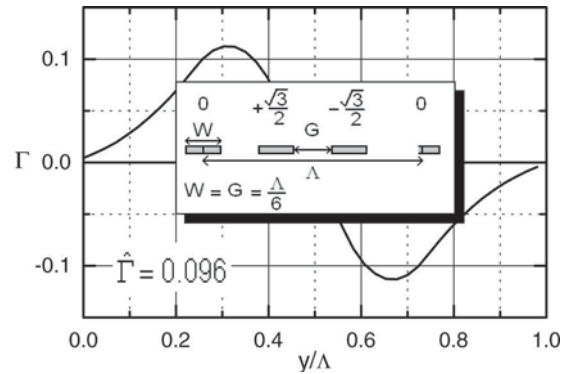


Fig. 5. Three-phase sine electrodes with corresponding driving voltages and local field overlap integral factors versus normalized local coordinate “ y .”

and $f(y)$ for one quadrature of the two-phase TE–TM mode converter. Figs. 4 and 5 show the two cases of the three-phase TE–TM mode converter with corresponding overlap integral factors $\Gamma(y)$ and structure function $f(y)$, respectively.

The resulting weighted overlap integral factors are $\hat{\Gamma} = 0.198$, 0.11, and 0.096, respectively. The two-phase $\hat{\Gamma}$ is resized to an effective value of $\sim 0.086 \dots 0.098$ if one takes into account that the two quadratures of the two-phase design need at least twice the length of the three-phase design. If the maximum permissible field strength limits the design, the factor V/G in κ , as defined in (4), is replaced by a constant. The three-phase design performs in its worst case (0.096) roughly equal or slightly better than the two-phase design. If the output range of the voltage sources is the limiting factor, κ is obtained through a multiplication by the same V/G ($8/\Lambda$, $9/\Lambda$, $6\sqrt{3}/\Lambda$), by which we have divided in calculating $\Gamma(y)$, as defined in (4). This yields equal κ values for both three-phase cases, and these are $1.26 \dots 1.44$, which are as high as κ in the two-phase case.

IV. LITHIUM NIOBATE TANTALATE (LNT)

This type of lithium niobate-based integrated optical PMDC should work up to at least 40 Gb/s. At 160 Gb/s, a poor performance is to be expected because the experimentally needed length for one full mode conversion is on the order of 5 mm. This means that the corresponding DGD of about 1.2 ps is only partly orientable. However, PMD compensation at 160 Gb/s or beyond seems to be mandatory to maximize dispersion-shifted fiber capacity, for example, in particular, in all Japan. To reach higher and higher bit rates, one needs to tailor the birefringence of lithium niobate. This is possible in principle in two ways: One possibility is to use a tilted waveguide in the YZ -plane, which will reduce the birefringence and, hence, the DGD. Tilted waveguide case has to be ruled out anyway because in tilted waveguides, propagation losses are rather high. This happens in tilted waveguides because the propagation constant of the guided mode and substrate radiation mode becomes identical. However, no attempt has been made to verify this argument independently, as it is clear from Sheem *et al.* [10] and Burns *et al.* [11]. The other possibility is to use the mixture of lithium niobate and lithium tantalate, which is also known as LNT.

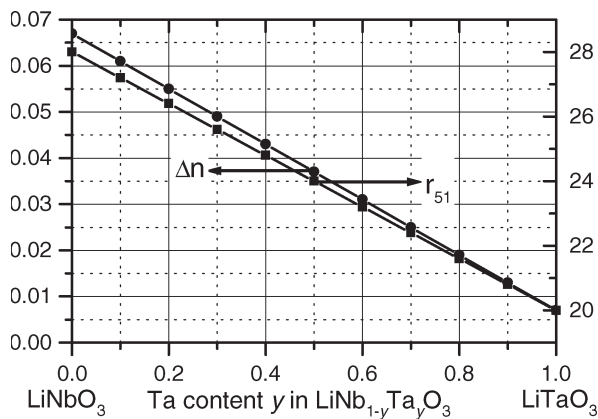


Fig. 6. Electrooptic coefficient r_{51} and Δn versus Ta content y in LNT crystals.

Mixed ferroelectrics have been the focus of intensive fundamental and applied research for many years. Interest in the study of these materials arises from the fact that the physical properties of crystalline materials are governed to a large extent by the composition of the crystals and, thus, can be tuned by varying the composition. One of the simplest ferroelectric mixed crystal systems is LNT, as both end members exhibit the same crystal structure (space group $R3c$) with only slight differences in the lattice and positional parameters. The physical properties can be very easily tuned by varying the parameter y in the composition of LNT crystals. To a certain degree, the mixed system yields a simple crystal modeling that may lead to well-functional materials and devices, which has direct implication for PMD compensation in optical communication systems.

Lithium niobate is slightly nonstoichiometric, typically Li-deficient, and preferably grown at the congruently melting composition with 48.5 mol% of Li_2O . A large variety of dopants ranging from +1 valent state H^+ to the +3 valent state such as rare Earth cations can be introduced into the crystal structure frame of lithium niobate. Most are known to occupy Li-sites. In contrast to these Li-site dopants, tantalum is isomorphic to niobium and replaces niobium when introduced into the crystal structure frame of lithium niobate. Tantalum can substitute niobium up to 100%. Any changes in the crystal composition will finally affect all physical properties of the crystal such as the linear dielectric response, i.e., refractive index, electrooptic coefficients, and so on. It has been shown in [12] that refractive index and electrooptic coefficients depend linearly on the Ta content y in LNT crystals. Therefore, one can tailor the birefringence of this mixed crystal, particularly for PMD compensation at higher bit rates [13].

The ordinary refractive index n_o and the relevant electrooptic coefficient r_{51} is shown in Fig. 6, which linearly depends on the Ta content y in LNT crystals:

$$\begin{aligned} n_o &= 2.2125 - 0.07 \cdot y \\ r_{51} &= 28 - 8 \cdot y. \end{aligned} \quad (5)$$

Fig. 7 shows the calculated optimum weighted field overlap integral factor $\hat{\Gamma}$, as defined above for two-phase, as well as two

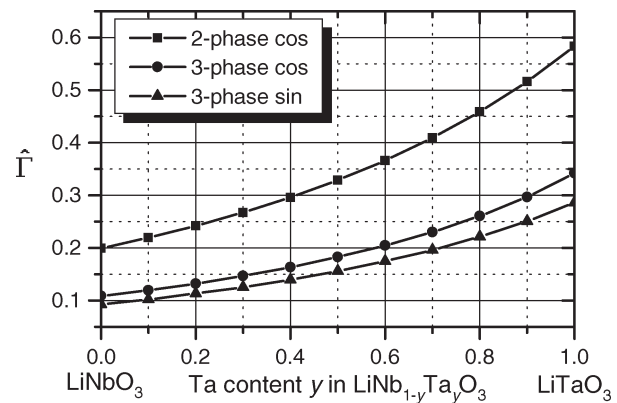


Fig. 7. Weighted field overlap integral factors versus Ta content y in LNT crystals.

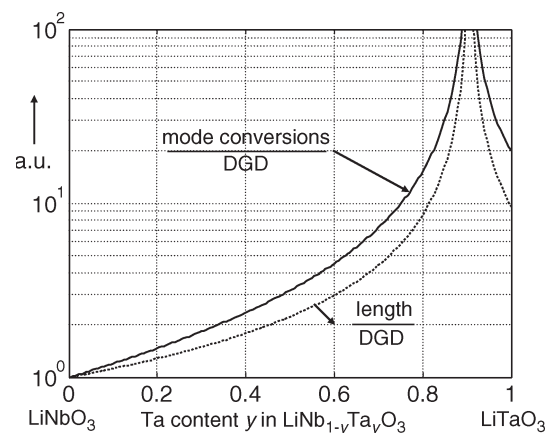


Fig. 8. Mode conversions/DGD and length/DGD for a given TE-TM mode converter versus Ta content y in LNT crystals.

representative cases of three-phase TE-TM mode converters with interdigital electrodes.

The numbers can be directly compared because the two-phase $\hat{\Gamma}$ has been halved due to the fact that the two-phase design needs at least twice the length of the three-phase design. Using this $\hat{\Gamma}$ and assuming two-phase electrodes, the achievable number of full mode conversions per DGD at electric field strength near breakdown ($10 \text{ V}/\mu\text{m}$) and the required length per DGD have been calculated as a function of the Ta content y in the LNT crystals (Fig. 8).

Pure lithium niobate allows for ~ 8 full mode conversions/ps in theory if $\hat{\Gamma} = 1$, and 0.8 full mode conversions/ps experimentally, in agreement with theory ($\hat{\Gamma} \approx 0.1$). Pure lithium tantalate allows for ≈ 20 times more mode conversions/DGD. The length/DGD is $\sim 4.2 \text{ mm}/\text{ps}$ in lithium niobate and $\sim 42 \text{ mm}/\text{ps}$ in lithium tantalate. However, this should not be problematic since less PMD may be expected in links for highest bit rates. Lithium tantalate alone should work in principle, up to at least 640-Gb/s operation. Appreciable advantages over pure lithium niobate with the potential of reaching 160-Gb/s operation can also be expected for low y , which may be accessible either by incorporating Ta into lithium niobate during crystal growth or later by thermal in-diffusion. An interesting situation occurs near $y = 0.9$, where the sign reversal of Δn promises terabit per seconds PMD compensation. A major problem for large y in LNT and pure lithium niobate are the large beat lengths,

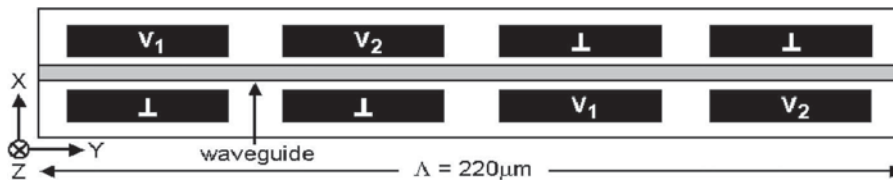


Fig. 9. Four-phase electrode structure for one period of TE-TM mode converter on Z-cut lithium niobate.

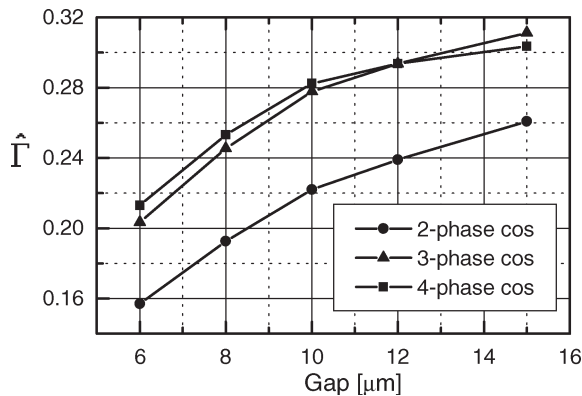


Fig. 10. Weighted field overlap integral factors versus gap in micrometers on Z-cut lithium niobate.

which scale proportional to the length/DGD. High voltages are required to reach fields near breakdown, even for three-phase electrodes, where the gaps are smaller (~ 370 V in lithium niobate).

V. Z-CUT LITHIUM TANTALATE

This problem is solved in Z-cut lithium tantalate. Fig. 7 shows the needed electrode pattern. Several periods will form one the in-phase and quadrature mode converter, and several mode converters will form a distributed PMDC. The voltage requirements are independent of the beat length Λ because the electric field perpendicular to the waveguide that is also parallel to the chip surface is decisive. Small gaps of $6 \dots 10 \mu\text{m}$ yield already large overlap factors but require modest voltages (110 V for $10 \mu\text{m}$, conveniently accessibly by 300-V transistors). The gaps between neighbor electrodes may be slightly wider than those across the waveguide. This is not a problem since Λ is large. Multiphase electrodes are therefore most efficient. An advantageous example is a four-phase design, which only needs two independent voltages to operate. Fig. 9 shows the schematic of such a scheme.

Fig. 10 shows the weighted field overlap factor $\hat{\Gamma}$ for representative voltage patterns as function of the gap in micrometers. The other cases, such as those shifted by $\Lambda/12$ for the three phase and by $\Lambda/8$ for the four-phase case, behave roughly equivalent. The four-phase outperforms the three-phase case, unless the lateral gap is so large that the compulsory longitudinal gaps consume too large a percentage of a period Λ . For a $10\text{-}\mu\text{m}$ gap, $\hat{\Gamma}$ is about the same (0.28) as for X-cut Y-propagation lithium tantalate. Therefore, we may expect ~ 16 mode conversions/DGD, which is ~ 20 times more than in lithium niobate, and this should be fine for up to 640-Gb/s operations.

VI. CONCLUSION

We found that a three-phase TE-TM mode converter can (but need not in all cases) outperform a two-phase converter. Tilting the waveguide in the YZ plane can drastically increase the efficiency, but the leaky mode's losses are the main issues involved in its realization. The other possibility is to use mixed ferroelectric crystals such as the LNT to realize high-bit rate PMDCs, where just a little DGD needs to be compensated. The birefringence Δn and electrooptic coefficient r_{51} decreases linearly with an increase of the Ta content y in LNT crystals. A Ta content y of up to 0.5 is good to realize a PMDC at about 160 Gb/s. An interesting situation occurs at $y = 0.9$, where the sign reversal of Δn opens up the possibility of terabit-per-second PMD compensation. This mixed ferroelectric solution to PMD compensation combines optimum performance and high speed with a high degree of integration and, hence, low-cost potential. Z-cut lithium tantalate is indeed suitable for PMD compensation up to 640-Gb/s operation. In Z-cut, voltage requirements are independent of the beat length, and four-phase electrodes are more attractive.

ACKNOWLEDGMENT

The authors would like to thank Prof. W. Sohler, Prof. K. Buse, and Prof. K. Betzler for useful discussions. The authors would also like to thank Dr. H. Hermann and R. Ricken for fabricating the PMDCs.

REFERENCES

- [1] R. Noé, D. Sandel, M. Yoshida-Dierolf, S. Hinz, V. Mirvoda, A. Schöpflin, C. Glingener, E. Gottwald, C. Scheerer, G. Fischer, T. Weyrauch, and W. Haase, "Polarization mode dispersion compensation at 10, 20, and 40 Gb/s with various optical equalizers," *J. Lightw. Technol.*, vol. 17, no. 9, pp. 1602–1616, Sep. 1999.
- [2] F. Heisemann and R. Ulrich, "Integrated optical single side band modulator and phase shifter," *IEEE J. Quantum Electron.*, vol. QE-18, no. 4, pp. 767–771, Apr. 1982.
- [3] D. Sandel and R. Noé, "Proposal for distributed polarization mode dispersion compensator in lithium niobate," in *Proc. ECIO*, Torino, Italy, Apr. 1999, pp. 237–240.
- [4] R. Noé, D. Sandel, S. Hinz, M. Yoshida-Dierolf, V. Mirvoda, G. Feise, H. Herrmann, R. Ricken, W. Sohler, F. Wehrmann, C. Glingener, A. Schöpflin, A. Färbert, and G. Fischer, "Integrated optical LiNbO₃ distributed polarization mode dispersion compensator in 20 Gb/s transmission system," *Electron. Lett.*, vol. 35, no. 8, pp. 652–654, Aug. 1999.
- [5] D. Sandel, V. Mirvoda, S. Bhandare, F. Wüst, and R. Noé, "Some enabling techniques for polarization mode dispersion compensation," *J. Lightw. Technol.*, vol. 21, no. 5, pp. 1198–1210, May 2003.
- [6] R. Noé, D. Sandel, and V. Mirvoda, "PMD in high-bit-rate systems and means for its mitigation," *IEEE J. Sel. Topics Quantum Electron.*, vol. 10, no. 2, pp. 341–355, Mar./Apr. 2004.
- [7] D. Marcuse, "Electrostatic field of coplanar lines computed with the point matching method," *IEEE J. Quantum Electron.*, vol. 25, no. 5, pp. 939–947, May 1989.

- [8] C. M. Kim and R. V. Ramaswamy, "Overlap integral factors in integrated optic modulators and switches," *J. Lightw. Technol.*, vol. 7, no. 7, pp. 1063–1070, Jul. 1989.
- [9] S. Bhandare and R. Noé, "Optimization of TE–TM mode converters on X-cut, Y-propagation LiNbO₃ used for PMD compensation," *J. Appl. Phys. B*, vol. 73, no. 5/6, pp. 481–483, 2001.
- [10] S. K. Sheem, W. K. Burns, and A. F. Milton, "Leaky-mode propagation in Ti-diffused LiNbO₃ and LiTiO₃ waveguides," *Opt. Lett.*, vol. 3, no. 3, pp. 76–78, Sep. 1978.
- [11] W. K. Burns, S. K. Sheem, and A. F. Milton, "Approximate analysis of leaky-mode loss coefficient for Ti-diffused LiNbO₃ waveguides," *IEEE J. Quantum Electron.*, vol. QE-15, no. 11, pp. 1282–1289, Nov. 1979.
- [12] D. Xue, K. Betzler, and H. Hesse, "Dielectric properties of lithium niobate–tantalate crystals," *Solid State Commun.*, vol. 115, no. 11, pp. 581–585, Aug. 2000.
- [13] S. Bhandare and R. Noé, "Pushing distributed PMD compensator performance toward highest bit rates by lithium niobate–tantalate or lithium tantalate crystals," presented at the 11th Eur. Conf. Integrated Optics (ECIO), Prague, Czech Republic, 2003, Paper WeA3.5.



Suhas Bhandare (M'05) was born in Nasik, India, in 1973. He received the M.Sc. and M.Phil. degrees in electronic science from the University of Pune, Pune, India, in 1995 and 1999, respectively, and the Ph.D. degree (Dr.Ing.) in electrical engineering from the University of Paderborn, Paderborn, Germany, in 2003.

He was a core member of the team that established the "Design and Engineering Center for Integrated Optics" at the Society for Applied Microwave Electronics Engineering and Research, Indian Institute of Technology Powai, Mumbai, India. At this center, he spent three years on the design, fabrication, and characterization of various types of integrated optical devices based on glass and lithium niobate. In 1999, he was with the Chair for Optical Communication and High-Frequency Engineering with the University of Paderborn as a Research Assistant. His research interests include phase-shift keying transmission at 40 Gb/s and beyond.

Dr. Bhandare is a Life Member of the Institution of Electronics and Telecommunication Engineers.



Reinhold Noé (M'93) was born in Darmstadt, Germany, in 1960. He received the Dipl.Ing. and Dr. Ing. degrees in electrical engineering from Technische Universität München, Munich, Germany, in 1984 and 1987, respectively. At that time, he realized the first endless polarization control systems.

Then, he spent a postdoctoral year at Bellcore, Red Bank, NJ, to continue his work on coherent optical systems. In 1988, he was with Siemens Research Laboratories in Munich. Since 1992, he has been heading the Chair of Optical Communication and High-Frequency Engineering with the University of Paderborn, Paderborn, Germany. Most of his recent experiments deal with polarization mode dispersion detection and compensation, polarization division multiplex, chromatic dispersion detection, differential quadrature phase-shift keying transmission (all at 40 Gb/s), and synchronous QPSK transmission. He has (co)authored more than 170 publications.

Dr. Noé is one of the Editors of *Electrical Engineering*, and he is a frequent referee for *Electronics Letters* and several IEEE publications.